İSTANBUL UNIVERSITY
CERRAHPAŞA

ORIGINAL ARTICLE
Electrica 2023; 23(3): 643-657

Comparison of Metaheuristic Optimization Techniques for the Optimal Placement and Sizing of Shunt Flexible Alternating Current Transmission Systems Device Considering Load Increase

Ghamgeen Izat Rashed[1,2], Duku Otuo-Acheampong[1,2], Akwasi Amoh Mensah[3], Hussain Haider[1,2]

[1]Hubei Engineering and Technology Research Center for AC/ DC Intelligent Distribution Network, School of Electrical Engineering and Automation, Wuhan University, Wuhan,China
[2]School of Electrical Engineering and Automation, Wuhan University, Wuhan, China
[3]Automation Science and Engineering and Automation, South China University of Technology, Guangzhou, China

Cite this article as: G. Izat Rashed, D. Otuo-Acheampong, A. Amoh Mensah and H. Haider, "Comparison of metaheuristic optimization techniques for the optimal placement and sizing of shunt flexible alternating current transmission systems device considering load increase," *Electrica*, 23(3), 643-657, 2023.

ABSTRACT

In this paper, the challenges of determining the optimal location and size of the flexible alternating current transmission systems (FACTS) devices on the transmission system are solved. The FACTS devices are placed and sized optimally using three optimizations: genetic algorithm, simulated annealing, and flower pollination algorithm (FPA). Three FACTS devices, capacitor, Static VAR Compensator (SVC), and static synchronous compensator (STATCOM), are determined for two parameters: location and size to solve the multi-objective problem. The simulation results are analyzed to find the best optimization and FACTS device to improve the voltage profile and simultaneously lower the active power loss of the system. To investigate its effectiveness, the proposed approach was tested using two test systems, Pakistan's transmission network and IEEE 30 bus. Conducted in three cases for the real system data, the first case being the base case with a 50% uniformly increase in both active and reactive power of the load bus voltage, the second case with a 50% increase in only the active power, and the third case with a 50% increase in reactive power. The comparison of this optimization has shown that FPA performed better than the other algorithm and with the fastest convergence rate. The simulation results demonstrate that STATCOM was effective to minimize the losses while enhancing the voltage profile. Also, the Wilcoxon test is applied to confirm the efficiency of the STATCOM device.

Index Terms—Flexible alternating current transmission systems device, load voltage deviation, metaheuristic optimization, total power loss, voltage stability.

I. INTRODUCTION

The electrical power sector has grown rapidly as a result of an increase in electrical power users and technological improvements. Because of the restructuring and deregulation of the energy supply market, the load demand on the transmission network rises, eventually leading to voltage collapse, bringing electric power transmission closer to its stability limits. These difficulties severely affect the system in numerous ways, such as overloading the transmission lines to operate beyond their loading limits. Designing and constructing new power plants or expanding the transmission lines to operate at maximum efficiency and reliability than before will be restricted due to limited resources and environmental limitations and will be expensive. Therefore, research on voltage stability is important to maintain system security [1].

Because most existing power transmission networks are alternating current (AC) grids, the flexible AC transmission systems (FACTS) device has provided an alternative approach to the power system, ensuring that it runs within its boundaries while requiring no major changes to the system design [2-3]. It also increases system transmission capacity, manages reactive power, increases the reliability of AC grids, reduces power transmission outages and high-load transmission line flow, and results in increased load capacity, operation, delivery, and production [4-6]. Due to the benefits and advantages that FACTS provide, placing it in the wrong location is of no benefit to the power system but rather increases the cost of production; therefore, there is a need to determine the best position and size in a power system to achieve its goals.

Corresponding author:
Ghamgeen Izat Rashed

E-mail:
ghamgeen@whu.edu.cn

Received: December 14, 2022

Accepted: June 12, 2023

Publication Date: July 20, 2023

DOI: 10.5152/electr.2023.22214

The trend of research in the last decade about FACTS devices is using various types of heuristic approaches to determine the size and location as discussed: Kavitha and Neela [7] study effort revealed the ideal arrangement of two FACTS devices static VAR compensator (SVC) and thyristor controlled series capacitor (TCSC). The number of FACTS devices, their placement, kind, and rating are all determined using particle swarm optimization (PSO), weight Improved particle swarm optimization (WIPSO), and biogeography-based optimization (BBO) approaches with the goal of improving line loadings and load voltage variations. In [8], the author used the PSO algorithm to place the device on IEEE 14-bus network. Fast voltage stability index and voltage collapse proximity index were used to determine the weak lines and buses for the optimal location of the devices to improve the voltage profile and increase real power transfer.

Bujal et al. [9] compared the performance of the gravitational search algorithm and its improved type for the placement and sizing of Distributed Generations (DG) impact on voltage stability margin, power loss minimization, minimum bus voltage, and total harmonic distortion on IEEE 64 system. For reactive power dispatch with loss and voltage deviation minimization, as the objective functions, an Artificial Bee Colony (ABC) algorithm technique was suggested in [10], which was expressed as a constrained optimization problem tested on IEEE 30 and 57 bus systems. Belati et al. [11] provide a method for improving the voltage profile while decreasing active power losses on the 118-test system. To discover the optimal location of SVC, the problem is presented as a mixed-integer nonlinear programming problem utilizing an optimal power flow. Various load levels and time periods are considered. The authors [12] assessed the voltage stability of the IEEE 39-bus test system using the Artificial Intelligence (AI) approach. In contrast to other indices, the authors [13] introduced the power system voltage stability index, which provides good performance and high accuracy in identifying voltage instability under various conditions, particularly in the real operation of the power system. Useful hybrid techniques, such as gradient-based and moth-flame algorithm in reference [14] are used to find the optimal location and size of TCSC, thyristor controlled phase shifter (TCPS), and SVC devices. The implementation was done on two bus systems, IEEE 14 bus and IEEE 30 using moth flame optimization (MFO) and JAYA blended MFO with the consideration of the installation cost [15].

Based on the literature review, all the methodologies are implemented on only IEEE standard data, and only few researches used more than two metaheuristic approaches for placing the FACTS devices which lacks sufficient accuracy and precision under different operation conditions and different loads. Another shortcoming of the literature is that there is no statistical analysis for the accuracy of the results. This study examines and determines the best placements and sizes for three FACTS devices [capacitor, SVC, and static synchronous compensator (STATCOM)] in order to increase the loadability limits of both the real power system and IEEE standard system while enhancing the voltage profile and decreasing real power losses. It does this by satisfying a number of physical and operational constraints, including generation and load balance, bus voltage limits, and active and reactive power limits, using three different heuristic optimization techniques. All the power flow simulation and optimization algorithm were done by using MATLAB software and with the MATPOWER package. A 132 kV transmission line of Peshawar Electric Supply Company (PESCO) in Pakistan is applied as a case study and to demonstrate and compare the efficiency of the methodology IEEE 30 bus system is used. This study uses a single-place FACTS device approach.

Following is an overview of the paper's main contributions:

- Providing a practical and theoretical comparison between simulated annealing (SA), genetic algorithm (GA) and flower pollination algorithm (FPA), which aims to determine the solution quality and efficiency in terms of computational time, while keeping a high degree of accuracy.
- Proposing an optimization approach based on three metaheuristics (GA, SA, and FPA) methods that work best for each FACTS device based on its characteristics for optimal sizing and placement in transmission network for various loading conditions and different network configurations.
- Determining an accurate solution for the best location and size of all the FACTS devices to solve the research objective function.
- Applying the proposed methodology on two test cases: real system data (Pakistan transmission system) and standard IEEE data (IEEE 30 bus) with objectives of minimizing voltage deviation and system real power loss.
- Present a well-known Wilcoxon signed rank statistical test of the FACTS controllers.

After the introduction, further contents of the paper are organized as follows: Modeling of the FACTS device is the second section, and the problem formulation is the third section. All metaheuristic optimization techniques were covered in the fourth section. The fifth part will discuss the simulation results and discussion and the Wilcoxon signed-rank test is discussed in the sixth section. The final section is conclusions.

II. MODELLING OF FACTS DEVICES

Because of their advantages, all of the FACTS devices used in this research are shunt-connected. These devices work as reactive power compensators, reducing system losses while boosting power transfer capability and improving static and transient stability [16].

A. SVC

As shown in Fig. 1, SVC is a shunt-connected device that comprises thyristor-controlled reactor (TCR) in parallel with a bank of capacitors that generate and absorb reactive power. It helps regulate the bus

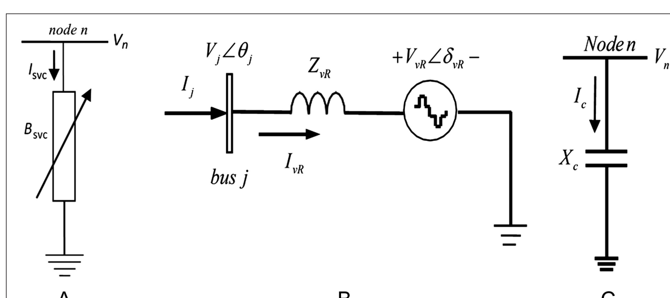

Fig. 1. (A) SVC, (B) STATCOM, and (C) shunt capacitor. It represents the model of the FACTS devices used in this paper. The first one is SVC, followed by STATCOM and the last is the shunt capacitor that is connected to node n. FACTS, flexible alternating current transmission systems.

voltage by compensating for the change of reactive power. From the figure, the current and reactive power by the SVC, which is also the reactive power supplied to bus n, is

$$I_{SVC} = jB_{SVC}V_n \tag{1}$$

$$Q_{SVC} = Q_n = -V_n^2 B_{SVC} \tag{2}$$

B. Static Synchronous Compensator

Fig. 1 presents a STATCOM, which works on the idea of a voltage source converter linked to the bus [17]. This device is used to control the voltage magnitude, reactive power injection and power flow, apparent power or current regulation, and voltage injection to the attached bus [18].

C. Shunt Capacitor

In transmission systems, shunt capacitors are utilized for reactive compensation, decreasing power loss, improving the voltage profile, and improving power flow [19]. The size of the capacitor at node n in Fig. 1 can be calculated as:

$$Q_c = V_n I_c \tag{3}$$

III. PROBLEM FORMULATION

Two fitness functions are used to express the problem to be solved: load voltage deviation and real power loss minimization. These fitness functions are optimized as a mono-objective function which is described later:

A. Objective Function

All the two-problem formulation will be performed individually as a mono-objective function minimization to be tested on the IEEE standard and real system transmission data with three different FACTS device using three metaheuristic algorithms while considering the equality and inequality constraints which is explained later:

1) Load Voltage Deviation (LVD)

The bus voltage deviation is affected by an increase in load in the electrical power system. The difference between the nominal and actual voltage is known as voltage deviation. LVD is used to minimize the value of the load voltage bus, which is defined later [7]:

$$LVD = \sum_{k}^{n} \left(\frac{V_k^{ref} - V_k}{V_k^{ref}} \right)^2 \qquad k = 1,2,\ldots,n \tag{4}$$

Where V_k^{ref} is the nominal voltage of 1 p.u., V_k represents the actual voltage magnitude at the load bus while n is the total number of load buses.

2) Total Active Power Loss

The transmission network's active power loss is described as follows [10]:

$$P_{Loss} = \sum_{i=1}^{N} g_{i,j} \left[V_i^2 + V_j^2 - 2V_i V_j \cos(\delta_i - \delta_j) \right] \tag{5}$$

where i and j are the indices from bus to bus, g is the conductance of transmission, N is the total number of feeders, V is the voltage magnitude of bus i or j, and δ is the angle of bus i or j.

B. System Constraints

There are two types of constraints related to this problem: equality and inequality constraints, which are stated as follows:

1) Equality Constraints

The equality constraints are the power flow equation calculated using the Newton–Raphson method. This is made up of the calculations of real and reactive power in each bus to determine the magnitude and phase angle.

$$P_{Gi} = P_{Di} + \sum_{j=1}^{N} V_i V_j \left(G_{ij} \cos(\delta_i - \delta_j) + B_{ij} \sin(\delta_i - \delta_j) \right) \tag{6}$$

$$Q_{Gi} = Q_{Di} + \sum_{j=1}^{N} V_i V_j \left(G_{ij} \sin(\delta_i - \delta_j) - B_{ij} \cos(\delta_i - \delta_j) \right) \tag{7}$$

where N is the total number of buses, P_{Gi} and Q_{Gi} represent the active and reactive power generated at bus i, P_{Di} and Q_{Di} are the active and reactive power load demand at bus i. $V_i V_j$ are the voltages at bus i and j. G_{ij} and B_{ij} are the real and imaginary part of an element *(i,j)* of the bus admittance matrix.

2) Inequality Constraints

The following are the constraints:

$$Q_{Gi}^{\min} \le Q_{Gi} \le Q_{Gi}^{\max}; \qquad i = 1,2,3,\ldots.,N_G \tag{8}$$

$$V_{Li}^{\min} \le V_{Li} \le V_{Li}^{\max}; \qquad i = 1,2,3,\ldots,N_{PQ} \tag{9}$$

$$S_l \le S_l^{\max}; \qquad l = 1,2,3\ldots,N_L \tag{10}$$

$$V_{Gi}^{\min} \le V_{Gi} \le V_{Gi}^{\max} \qquad i = 1,2,\ldots,N_{PV} \tag{11}$$

$$t_i^{\min} \le t_i \le t_i^{\max} \qquad i = 1,2,\ldots,N_T \tag{12}$$

$$Q_{ci}^{\min} \le Q_{ci} \le Q_{ci}^{\max} \qquad i = 1,2,\ldots N_C \tag{13}$$

$$P_{Gi}^{\min} \le P_{Gi} \le P_{Gi}^{\max} \qquad i = 1,2,\ldots N_{PV} \tag{14}$$

$$\delta_{ij}^{\min} \le \delta_{ij} \le \delta_{ij}^{\max} \qquad i = 1,2,\ldots,N \tag{15}$$

$$P_{ij} \le P_{ij}^{\max} \qquad i = 1,2,\ldots N_l \tag{16}$$

where V_{Li} represent the bus voltage, Q_{Gi} is the reactive power of generator buses, $S_l^{\max}$ is the maximum apparent power flow in line *l*. N_{PQ}, N_G, and N_L represent the number of load buses, generator buses, and transmission line. N_C is the number of compensating devices, N_T is the number of transformers, V_{Gi} is the voltage at generator bus *i*, P_{Gi} and Q_{Ci} represent the real and reactive power of generator at bus *i*, t_i is the tap ratio of the transformer, δ_{ij} is the voltage angle difference between bus *i* and *j*, P_{ij} shows the power flow in a line connected between bus *i* and *j*.

IV. METAHEURISTIC OPTIMIZATION TECHNIQUES

A. Genetic Algorithm

GA is a metaheuristic optimization developed by John Holland [20]. The concept of this stochastic global search method is to mimic the principles of natural genetics. The analysis for the devices, shunt capacitor, SVC, and STATCOM are done separately, and their results are compared later. The working principles are made up of three parameters: selection, crossover, and mutation rate applied at each iteration. The steps involved in the implementation of the GA are as follows:

1) Initialization

GA implementation begins with an optimization problem represented by an initial randomly generated population. The population consists of large individual configurations based on the FACTS device and is encoded in two parameters: location and size. The FACTS devices must be placed at the load buses and not the generator buses.

2) Fitness Function

This is derived based on the objective function in (4) and (5), which measures each individual's performance of the current population to minimize the active power loss and maintain the bus voltages closer to their allowable limit. However, the objective function independently checks the performance of a particular set of genes. A high fitness value indicates the greater quality of the solution according to this expression:

$$F(x) = \frac{1}{1+f(u)} \tag{17}$$

where $F(x)$ is the fitness function and $f(u)$ is the objective function.

3) Selection

The Roulette wheel method is chosen during the selection stage. It is based on the stochastic method, used to determine the number of individuals selected for reproduction based on the fittest survival principle from the fitness function. This selection method works by allocating segments to individuals of the population based on the proportion of the individual's relative fitness scores. After successive spinning of the wheel, parents will be selected based on the probability of the individual fitness:

$$P_i = \frac{F(x)}{\sum_{k=1}^{N} F(x_k)}, \qquad i = 1,2,...,N \tag{18}$$

where N is the size of the population and $F(x)$ is the fitness function. Producing of the population for the next generation is taken from two chromosomes with the highest fitness.

4) Crossover

After selecting the two chromosomes, the next stage is the crossover operation. Due to the large population, a two-point crossover is used. Only two points on the parent chromosome are selected with this method, and the other points are exchanged. This new chromosome shares the same characteristics of both parents' genetic material.

5) Mutation

To generate the offspring, only one parent is required in this stage. The substitution operation method was used as the mutation operator to change one random position of the chromosome and replace the corresponding gene, with a probability of the mutation being:

$$P_m = \frac{1}{T\sqrt{l}} \tag{19}$$

where T is the total generation number and l is the chromosome length.

6) Termination Criteria

The algorithm finally stops after the termination condition is achieved, displaying the best location and size of the FACTS device.

B. Flower Pollination Algorithm

FPA is a metaheuristic optimization whose techniques is based on nature phenomena. It was developed by Xin-She Yang in 2012 inspired by the pollination process of flowering plants [21-23]. The idea was based on pollination, which occurs in flowering plants with the transfer of pollens. They are of two types [24], self-pollination and cross-pollination. Self-pollination represents 10% of all flowering plants where the pollens are transferred from the same flowering plant or from another flower on the same plant and cross-pollination takes 90% of flowering plants where the pollen is transferred from one plant to another by a pollinator, such as an insect, wind, etc.

This algorithm makes use of four rules for its working principles [24]:

Rule 1: Cross-pollination is regarded as the algorithm's Levy flight satisfying global search procedure that obeys Levy flight.

Rule 2: The algorithm's local search function is caused by self-pollination.

Rule 3: Flower constancy, the likelihood of flower reproduction is proportional to how closely the two flowers that are being pollinated resemble one another.

Rule 4: Global and local search is controlled by switch probability between 0 and 1.

These rules are formulated into mathematical equation for global optimization. Each plant has a single flower with pollens, but each pollen is a potential solution to the objective function.

Equation (20) represents the global search and flower constancy by combining both rules 1 and 3:

$$S_i^{t+1} = S_i^t + \gamma_1 L(\lambda)\left(G^* - S_i^t\right) \tag{20}$$

*G** is the current best position where the global optimal solution is located. The S_i^t indicating the solution vector at the t-th iteration, *L* is the step size derived from the *Lévy* flight distribution that corresponds to the strength of the pollination which is calculated using (21), and γ_1 is the step size scaling factor which is 0.1.

$$L : \frac{\lambda\Gamma(\lambda)\sin(\pi\lambda/2)}{\pi}\frac{1}{z^{1+\lambda}}, (z ? z_0 > 0) \tag{21}$$

where $\Gamma(\lambda)$ is the standard gamma function of $\lambda = 1.5$ [21] and *v* indicates the step size by using (22)

$$z = \frac{\mu}{|v|^{\frac{1}{\lambda}}}, \mu : (0,\sigma^2), v : N(0,1) \tag{22}$$

where μ and *v* are random number subject to Gauss distribution. μ is the distribution with the mean zero variance of σ^2. The parameter σ is calculated as [21].

$$\sigma^2 = \left[\frac{\Gamma(1+\lambda)}{\lambda\Gamma\left(\frac{1+\lambda}{2}\right)} \cdot \frac{\sin\left(\frac{\lambda}{2}\pi\right)}{2^{\frac{\lambda-1}{2}}} \right]^{\frac{1}{2\lambda}} \quad (23)$$

Rules 2 and 3 are combined as the local search pollination expressed in [21]. FPA's convergence is improved by this operator.

$$S_i^{t+1} = S_i^t + \varepsilon\left(S_j^t - S_k^t\right) \quad (24)$$

where S_j^t and S_k^t are random generated values, and ε is a value in uniform distribution between 0 and 1. The last FPA rule is switch probability. This percentage influences whether the pollination selection is made using local or global search [21]. For the local best operator, the probability coefficient (P) is equal to .8, while it is equal to .2 for the global best operator.

1) *FPA Implementation*

With this optimization, to minimize the power losses and enhanced the voltage deviation of the system, the flower is considered as the control variable, namely the locations and size of the FACTS devices. The fitness of the flower is determined by the objective function during the load flow which displays the locations and size of the devices that comes with the minimized losses and voltage deviations.

The implementation of this algorithm is as follows:

Step 1: Initialize the parameters such as the iteration number t, initial population size N, switch probability of flower pollination $P = .8$, and Levy's flight step size.

Step 2: Initialize the population.

Step 3: Compute the objective functions using (4) and (5).

Step 4: The best solution is identified in the initial population as g*.

Step 5: Begin iteration by setting t = 1.

Step 6: Cross-pollination activity is carried out if rand > p; else, self-pollination is carried out.

Step 7: The step size L is computed using (21), and a new solution is obtained with (20)

Step 8: Draw evenly from the distribution and select solutions j and k at random from the population instead of i. Use (24) to create a new solution for i.

Step 9: A new solution for the objective function is computed, and replaces the old solution in step 3 if is better than that if not repeat steps 3 to 9 for all i.

Step 10: Verify termination criterion.

Step 11: Display the result (location and size).

C. Simulated Annealing

SA, a metaheuristic optimization method, was proposed in 1953 [25] as a modified Monte Carlo integral method. Later, it was generalized by Kirkpatrick, Gelatt, and Vecchi in 1983 as an algorithm that uses temperature as its controlled parameter [26]. This optimization method uses an annealing process, a metallurgical procedure of heating a metal to a high temperature until it melts. It cools gradually by reducing the temperature in stages to gain the desired shape, thus minimizing the system energy since this optimization method aims to get the best metallic crystal. SA comprises two stochastic processes: that is, generation and acceptance of the solution.

The optimal solution is acquired in SA through random search and iteration methods. The purpose of this work is to determine the best location and size for FACTS devices on the buses to minimize real power loss and keep the voltage within acceptable limits. To apply the algorithm, these steps will be followed:

1. First, we configured the FACTS devices with these parameters: the location and size since the algorithm will be run separately for each device and compare the results.
2. An initial random solution and a high value of temperature are generated.
3. New solution points are generated randomly near the current point.
4. Implement the objective function in (4) and (5). The algorithm compares the new solution's objective function against the present solution's objective function. If the new solution's objective function is lower than the existing solution, it is accepted and becomes our next solution; if it is higher, the algorithm will accept it based on this probability of acceptance, which is compared to a randomly generated number between 0 and 1. $P = e^{-\Delta J/kT}$, $\Delta J =$ where the new objective − old objective, k represents the Boltzmann's constant, and T as the current temperature. The next solution is accepted when the random number is less than P with this probability.
5. Methods of cooling: The algorithm lowers the cooling control parameter as $T_{k+1} = \alpha T_k$, where α is the temperature decrement factor $0 < \alpha < 1$. The temperature has to be slowly controlled to generate a better solution and faster convergence.
6. Stopping criteria. The algorithm stops after it is satisfied with the objective function of locating and sizing the FACTS devices.

V. SIMULATION RESULTS AND DISCUSSION

In order to implement all the metaheuristic approaches to analysis for its effectiveness, a real system and IEEE standard bus system are used as the test case to find the optimal location and sizing of the capacitor, SVC, and STATCOM. Single-type FACTS device allocation methodology will be used in this research, where all the proposed GA, FPA, and SA algorithms will be run separately for each FACTS device and the results are compared to determine the best optimization that works perfectly for them. Then based on those results, a conclusion will be drawn on the FACTS device that was effective to get the lowest real power loss minimization and reduces the voltage deviation as well. The control parameters of the optimization techniques used in this study are shown in Table I. The load flow analysis and optimization programming were performed with the use of MATPOWER toolbox package [27] using the Newton–Raphson method in the MATLAB software.

The simulation will be performed on 132 kV transmission line of PESCO and IEEE 30 bus system which is discussed later.

A. IEEE 30 Bus System

This bus system consists of 6 generator buses, 30 buses, 24 load buses, 4 transformers, and 41 transmission lines given in the MATPOWER

TABLE I. CONTROL PARAMETERS OF GA, FPA, AND SA

Name of the Parameter	GA	FPA	SA
Population size (*n*)	50	30	—
Maximum generation	200	—	—
Crossover probability (Pc)	0.8	—	—
Mutation probability	0.02	—	—
Type of selection	Roulette wheel	—	—
Type of crossover	Two-point	—	—
Maximum number of iteration	300	300	300
Switching probability (*P*)	—	0.8	—
Scaling parameter (γ)		0.1	
Initial point	—	—	0
Initial temperature	—	—	100
Reanneal interval	—	—	50

FPA, flower pollination algorithm; GA, genetic algorithm; SA, simulated annealing.

toolbox [27]. With a total generation capacity of 191.6 MW and 100.4 MVAr, the total load connected is 189.2 MW and 107.2 MVAr.

1) Comparison of Results for Voltage Profile Improvement

As shown in Table II, all the details of the optimization techniques used for the placement of the FACTS devices are listed there. Focusing on minimizing the bus voltage deviation, the STATCOM device had the lowest reductions compared to the capacitor and SVC with the use of FPA techniques from the based case of 0.0138 p.u. to 0.0068 p.u. as shown in Fig. 2.

2) Comparison of Results for Total Active Power Loss

From Table II, all the various optimization techniques successfully reduced the real power losses of all the FACTS devices. Without the placement of the FACTS devices, the losses were 2.444 MW but with the use of the shunt capacitor connected to bus 10, FPA had the lowest reduction of 2.1700 MW while placing SVC at bus 6 with a reactive power of 43 MVAr with FPA techniques had P_{loss} of 1.8521 MW. As shown in Fig. 3, with all the FACTS, STATCOM had the lowest active loss when connected to the optimal location using all three techniques with the FPA technique being the best with 1.58483 MW.

Comparing the performance of all the algorithms, Fig. 4 Fig. 5 Fig. 6 display the convergence characteristics of all the algorithms applied on all the devices; in all cases, FPA convergences faster with fewer iterations to reach an optimum value, followed by the GA.SA always displayed the worst convergence speed.

B. PESCO Bus Systems

To assess the suggested methods for installing the FACTS device to prevent voltage collapse, the data and parameters used in this study are acquired from Pakistan. Due to the large network in the country, we focus on the part of the 132 kV transmission line of PESCO and not all. PESCO provides electricity to Peshawar, Mardan, Bannu, Malakand, Dera Ismail Khan, Hazara, and Kohat civil divisions. PESCO had a transmission loss of 386 GWh on the 132 kV line, and it is projected to increase every year; as a result, there is a need to research how to make the voltage stable. The 132 kV PESCO bus network is a real system data consisting of 3 generators, 39 buses, 50 branches, and 15 loads, as shown in Fig. 7. With a total generation capacity of 264.2 MW and 201.1 MVAr, total load connected is 283.4 MW and 126.6 MVAr.

The load power will be increased uniformly at each load bus to assess the variation of load conditions and its effects on the transmission line. This simulation is divided into three categories for ease of understanding: case 1 is the base load scenario, case 2 is the load active power increment, and case 3 is the load reactive power increment. Each case will have a load increase of 50%, which is discussed later:

C. Comparison of Results for Voltage Profile Improvement

The goal is to enhance the voltage profile, decrease the load voltage variation, as shown by the objective function in (4), and maintain the load bus voltage within the nominal voltage range. All detailed simulations performed are listed in Table III to Table VI. Showing the optimization of each device on a graph will be a lot, so due to simplicity, in each graph, the effective optimization is selected for the capacitor, SVC, and STATCOM for comparison.

TABLE II. RESULTS AND COMPARISONS OF FACTS DEVICE USING GA, SA, AND FPA OF THE IEEE BUS SYSTEM

Base Case										
		Capacitor			SVC			STATCOM		
	Base	GA	SA	FPA	GA	SA	FPA	GA	SA	FPA
Location		17	9	10	8	6	6	26	28	26
Size		87.325	99.858	88.014	43.514	50.214	43.021	37.241	43.012	30.774
V_{min} (p.u.)	0.9606	0.9664	0.9660	0.9664	0.9679	0.9608	0.9677	0.9679	0.9701	0.9679
V_{max} (p.u.)	1	1	1	1	1.0125	1	1	1.0318	1.0051	1
LVD (p.u.)	0.0138	0.0115	0.0116	0.0111	0.0097	0.0099	0.0096	0.0072	0.0075	0.0068
P_{loss} (MW)	2.444	2.1731	2.1848	2.1690	1.8624	1.8801	1.8521	1.6216	1.589	1.5848

FACTS, flexible alternating current transmission systems; FPA, flower pollination algorithm; GA, genetic algorithm; SA, simulated annealing.

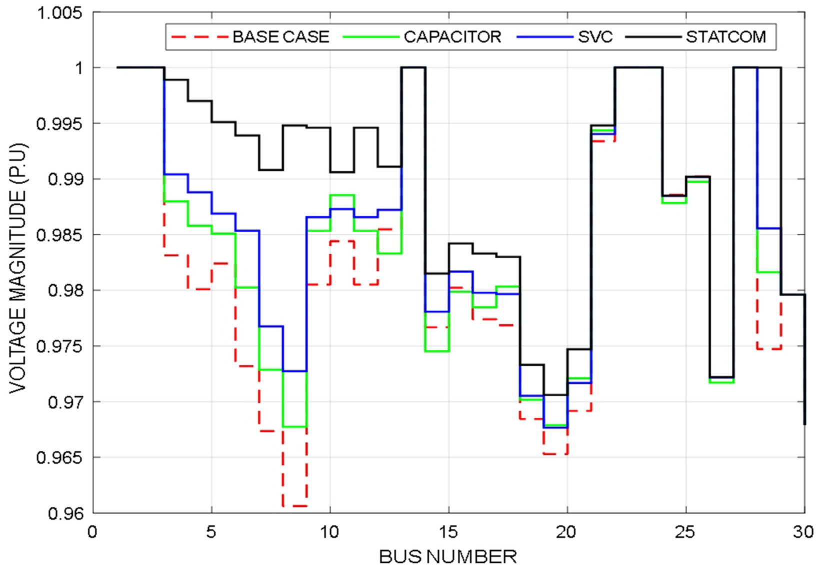

Fig. 2. Voltage profile comparison of IEEE 30 Bus system. All three devices (capacitor, SVC, STATCOM) are compared for the voltage profile of the bus system. The FPA algorithm was used for the plot because it was effective when compared to the GA and SA. FPA, flower pollination algorithm; GA, genetic algorithm; SA, simulated annealing.

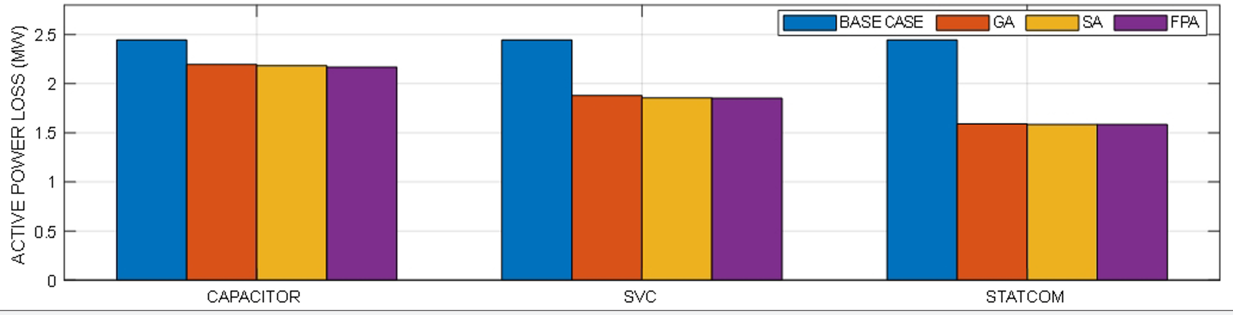

Fig. 3. Active power loss of IEEE 30 bus system. Reducing the active power loss of the 30-bus system, capacitor, SVC, and STATCOM devices were used. Each device's location and size were determined using three optimizations (GA, SA, and FPA). In this plot, FPA algorithm was plotted because it was effective as compared to the others. FPA, flower pollination algorithm; GA, genetic algorithm; SA, simulated annealing.

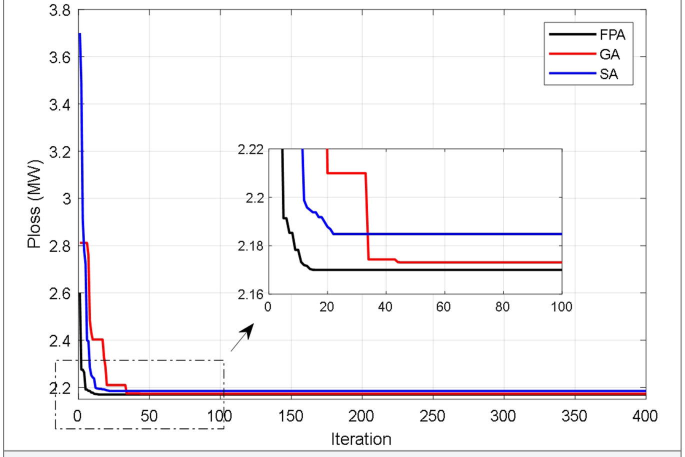

Fig. 4. Convergence curve of P_{loss} for the capacitor. To analyze the performance of each algorithm by using a capacitor, the convergence curve is plotted when used for the minimization of the real power losses on the IEEE 30 bus system.

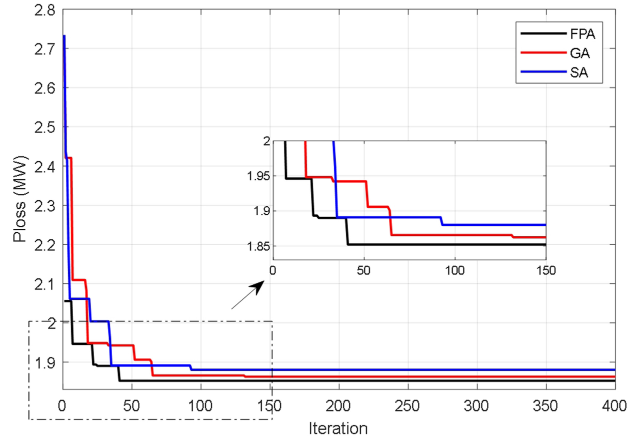

Fig. 5. Convergence curve of P_{loss} for the SVC. To analyze the performance of each algorithm by using SVC, the convergence curve is plotted when used for the minimization of the real power losses on the IEEE 30 bus system.

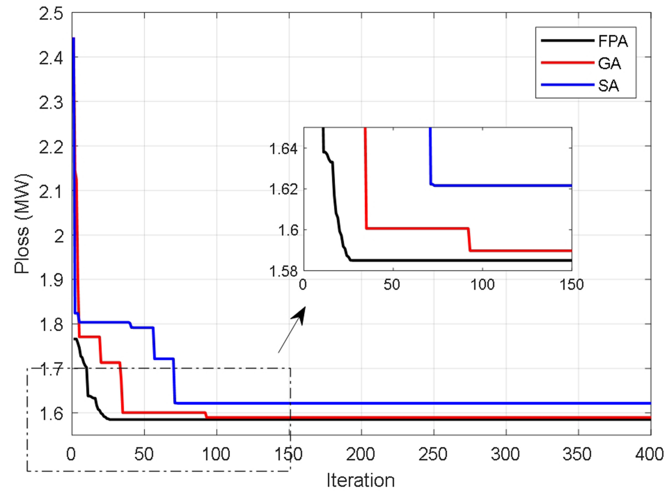

Fig. 6. Convergence curve of P_{loss} for the STATCOM. To analyze the performance of each algorithm by using STATCOM, the convergence curve is plotted when used for the minimization of the real power losses on the IEEE 30 bus system.

1) Case 1 (Base Case)

This is the same as the test case. Table III shows the detailed solution of the algorithm with the use of GA, SA, and FPA algorithms for the placement of capacitor, SVC, and STATCOM. Using a single-type FACTS device, the graph in Fig. 8 shows the relation of the device compared to the base case; the capacitor reduces the voltage deviation from 0.148 to 0.1152, and SVC further reduced it to 0.0137 with both using FPA optimization. STATCOM, connected in shunt with bus 15, drastically reduced it to 0.0082 at each load bus within the acceptable voltage magnitude of 0.95 to 1.05 p.u.

Both active and reactive power of the load bus were uniformly increased to 50% to examine the effects of load increase on the power system. As presented in Table IV, after the load flow, the voltage deviation is 0.45222 with V_{min} of 0.8264 and 1 V_{max}. In Fig. 9, injecting a reactive power of 360.066 kVAR to bus 8 using a capacitor reduces the voltage deviation to 0.2223 but with a V_{min} of 0.8868. The SVC regulated the voltage at 0.05003 on bus 24, but all bus voltage was not within the acceptable range. 80 MVAr was injected to bus 29 by STATCOM with a minimum voltage magnitude of 0.95 and V_{max} of 1.0215 to boost the voltage profile to 0.0172 p.u.

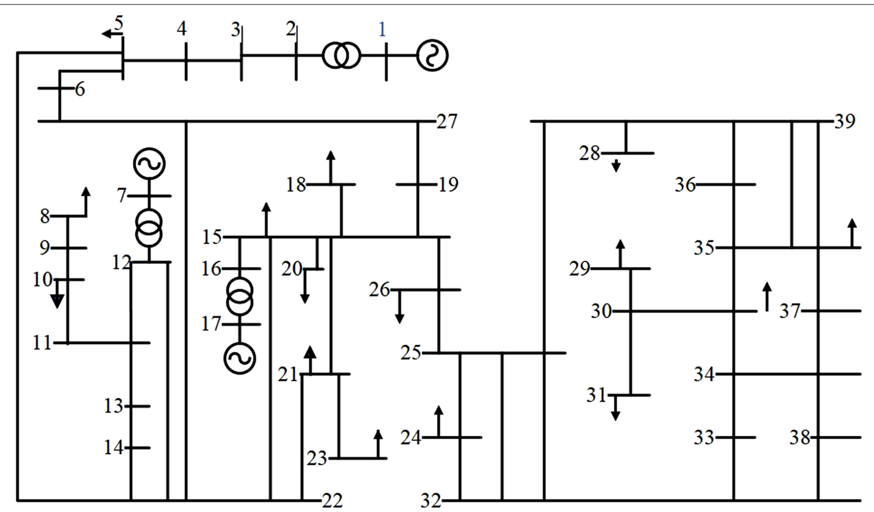

Fig. 7. 132 kV Peshawar Electric Supply Company (PESCO) transmission line. The transmission line of 132 kV PESCO is shown in this figure. This transmission line is just a portion of the whole network used in this research for the analysis of voltage stability with the primary focus on loss reduction and voltage enhancement on the buses.

TABLE III. RESULTS AND COMPARISONS OF FACTS DEVICE USING GA, SA, AND FPA OF THE TEST SYSTEM

	Base Case									
		Capacitor			SVC			STATCOM		
	Base	GA	SA	FPA	GA	SA	FPA	GA	SA	FPA
Location		29	30	24	10	20	24	15	29	15
Size		301.074	310.928	300.372	83.456	88.799	82.982	66.113	72.502	66.634
V_{min} (p.u.)	0.900	0.9138	0.9107	0.9145	0.9439	0.9402	0.9439	0.9753	0.9549	0.9585
V_{max} (p.u.)	1	1	1	1	1.0195	1.0169	1.0196	1.0424	1.0239	1.0193
LVD (p.u.)	0.148	0.1168	0.1214	0.1152	0.013725	0.0185	0.0137	0.0089	0.0107	0.0082
P_{loss} (MW)	11.216	10.359	10.548	9.8015	9.68057	9.7834	8.854	8.0022	6.2095	5.6963

FACTS, flexible alternating current transmission systems; FPA, flower pollination algorithm; GA, genetic algorithm; SA, simulated annealing.

TABLE IV. RESULTS AND COMPARISONS OF FACTS DEVICE USING GA, SA, AND FPA OF THE TEST SYSTEM (50% LOAD INCREASE)

		Base Case (50%)								
		Capacitor			SVC			STATCOM		
	Base	GA	SA	FPA	GA	SA	FPA	GA	SA	FPA
Location		20	24	8	24	29	24	29	29	29
Size		364.354	370.185	360.066	107.124	110.689	107.109	82.656	84.561	80.009
V_{min} (p.u.)	0.8264	0.8861	0.8692	0.8868	0.8997	0.8934	0.9025	0.91605	0.9153	0.9500
V_{max} (p.u.)	1	1	1	1	1.03798	1	1.0213	1.01994	1.0151	1.0215
LVD (p.u.)	0.45222	0.22416	0.25080	0.2223	0.06496	0.16212	0.05003	0.03212	0.0341	0.0172
P_{loss} (MW)	44.1204	37.2102	34.2188	28.9428	21.6062	21.6062	21.5091	19.7022	19.0017	18.9033

FACTS, flexible alternating current transmission systems; FPA, flower pollination algorithm; GA, genetic algorithm; SA, simulated annealing.

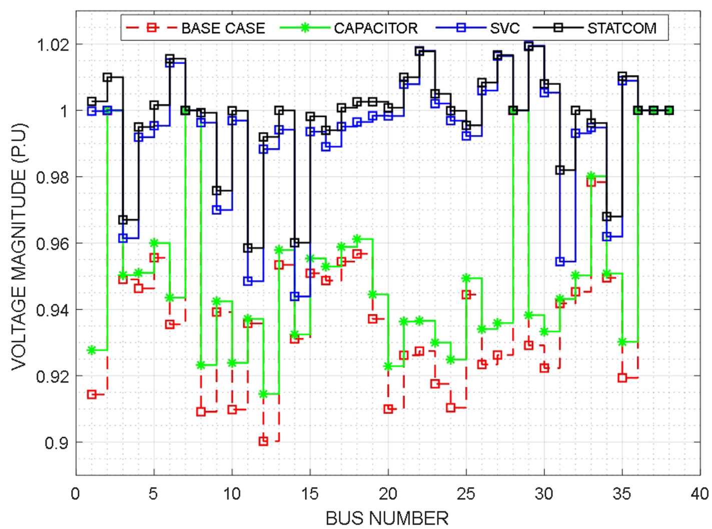

Fig. 8. Voltage profile comparison of base case. For the comparison of all bus's voltage magnitude deviation, GA, SA, and FPA was applied on all three FACTS devices for its optimal location and sizing. This plot only displays the method that was effective to enhance the deviation which was FPA in all devices when analyzing the base case. FACTS, flexible alternating current transmission systems; FPA, flower pollination algorithm; GA, genetic algorithm; SA, simulated annealing.

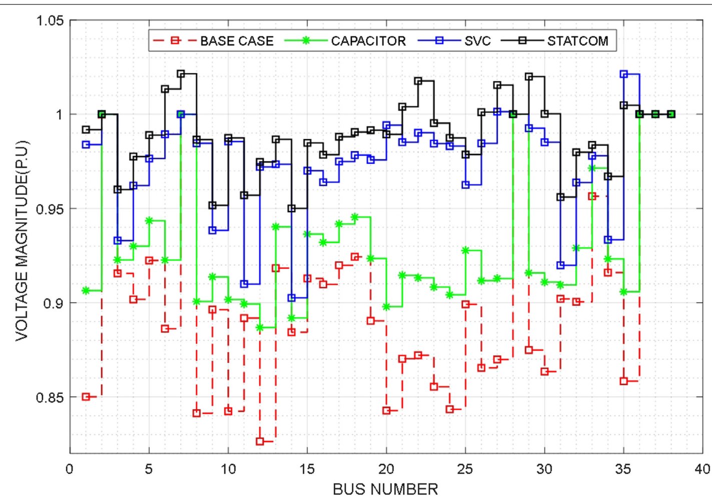

Fig. 9. Voltage profile comparison of 50% load increase. All three devices (capacitor, SVC, and STATCOM) are compared for the voltage profile of each bus in this transmission system when both real and reactive power load is increased to 50% of the base case. The FPA algorithm was used for the plot because it was effective when compared to the GA and SA. FPA, flower pollination algorithm; GA, genetic algorithm; SA, simulated annealing.

TABLE V. RESULTS AND COMPARISONS OF FACTS DEVICE USING GA, SA, AND FPA OF THE TEST SYSTEM (50% P_{LOAD} INCREASE)

P_{load} Increase (50%)										
		Capacitor			SVC			STATCOM		
	Base	GA	SA	FPA	GA	SA	FPA	GA	SA	FPA
Location		35	20	24	8	35	24	29	24	29
Size		394.825	399.2324	390.729	112.301	117.437	113.713	85.610	100.701	83.996
V_{min} (p.u.)	0.8695	0.8946	0.9101	0.9187	0.9241	0.9199	0.9241	0.9403	0.9397	0.9501
V_{max} (p.u.)	1	1	1	1	1.0042	1.000	1.0054	1.0264	1.0538	1.0147
LVD (p.u.)	0.2609	0.1541	0.1279	0.1091	0.038707	0.07314	0.03558	0.017	0.0193	0.0134
P_{loss} (MW)	34.4215	28.577	26.39672	26.0021	19.4849	16.7485	16.571	15.5326	15.0326	13.7553

2) Case 2 (P_{load} Increase)

In this case, only the real power of all the load bus in the base case is increased. It is increased to 50% uniformly with an LVD of 0.2609 p.u., as shown in the 8th row of Table V. Visibly shown in Fig. 10, the FPA optimization technique placed the STATCOM at bus 29 to generate a reactive power of 83.996 MVAr, thereby reducing the voltage deviation drastically to 0.0134 p.u. with V_{min} of 0.9501 p.u. and V_{max} of 1.0147 p.u. followed by SVC with 0.03558 p.u. and 0.1091 p.u. for the capacitor.

3) Case 3 (Q_{load} Increase)

Performing the load flow analysis after increasing the reactive power of all the load bus by 50%, the tabulated results are displayed in Table VI with an LVD of 0.286085 p.u.; with the placement of the FACTS device, each device was able to improve the voltage deviation. However, from the graph in Fig. 11, placing STATCOM at bus 29 injected a reactive power of 81.410 MVAr with the use of FPA optimization yielded a better result at a voltage deviation of 0.0151 p.u., and all buses were within their permissible limit that is between 0.95 p.u. and 1.05 p.u.

D. Comparison With Solutions for Total Active Power Loss

In this part, the system's load voltage is increased, and a simulation is run for the base case and after the shunt-connected FACTS devices are installed to examine the Total Power Losses solely.

1) Case 1 (Base Case)

After the load flow, before the placement of the FACTS device, the total active loss is 11.216 MW in Table III. After the placement of the FACTS device, all optimization technique is plotted as shown in Fig. 12. With the shunt capacitor and SVC in the base case, FPA optimization effectively reduced the total active loss with a smaller size than the other optimizations. However, this reduction was not the minimum, although SVC was better than the shunt capacitor, with the excellent work of the STATCOM in improving the voltage profile, it also reduces the total active power loss to 5.6963 MW when it is placed at bus 15 with the help of the FPA algorithm.

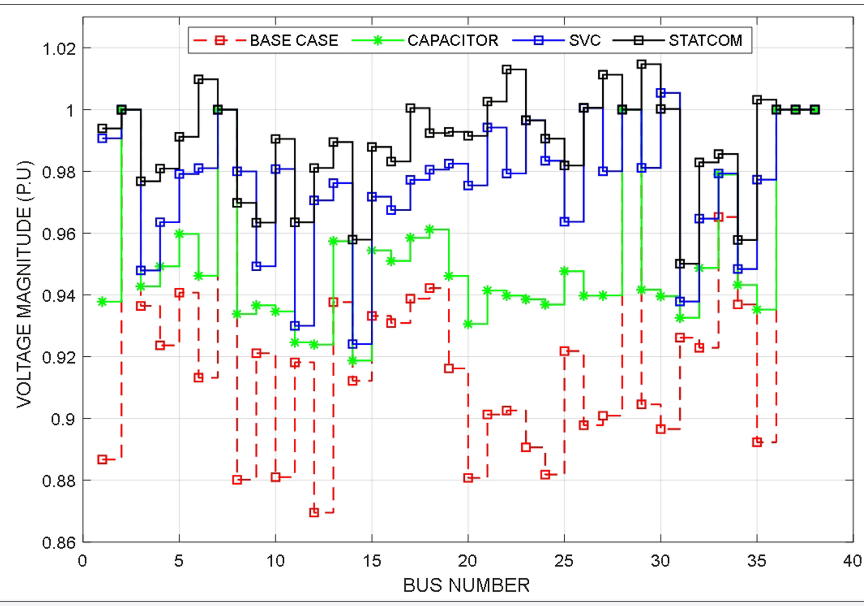

Fig. 10. Voltage profile comparison of 50% P_{load} increase. All three devices (capacitor, SVC, and STATCOM) are compared for the voltage profile of each bus in this transmission system when only the real power load is increased to 50% of the base case. This plot only displays the method that was effective to enhance the deviation which was FPA in all devices when analyzing the base case. FPA, flower pollination algorithm.

TABLE VI. RESULTS AND COMPARISONS OF FACTS DEVICE USING GA, SA, AND FPA OF THE TEST SYSTEM (50% Q_{LOAD} INCREASE)

Q_{load} Increase (50%)										
		Capacitor			SVC			STATCOM		
	Base	GA	SA	FPA	GA	SA	FPA	GA	SA	FPA
Location		15	8	29	20	8	24	29	21	29
Size		203.489	208.971	201.032	106.5425	108.689	106.115	85.263	90.023	81.410
V_{min} (p.u.)	0.860206	0.87606	0.86792	0.8779	0.9177	0.91427	0.9181	0.9344	0.930551	0.9500
V_{max} (p.u.)	1	1	1	1	1	1	1.0210	1.03488	1.013138	1.0300
LVD (p.u.)	0.286085	0.23491	0.2618	0.23326	0.0466	0.0568	0.034	0.02252	0.0226	0.0151
P_{loss} (MW)	17.10405	15.421	15.379	15.0071	14.9879	14.9159	13.818	13.7498	12.68075	10.731

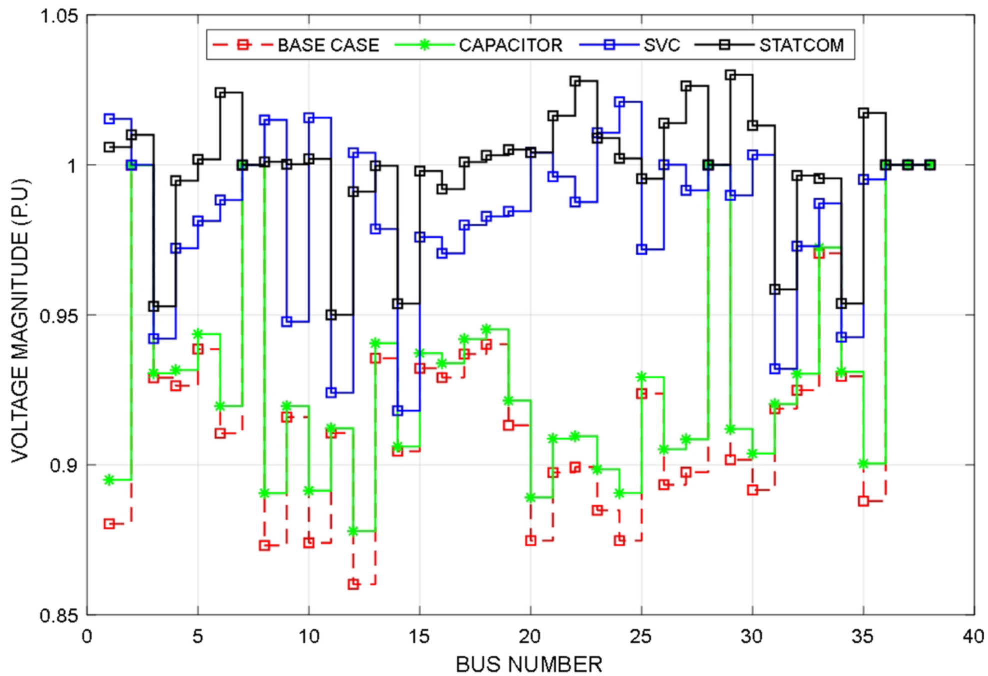

Fig. 11. Voltage profile comparison of 50% Q_{load} increase. All three devices (capacitor, SVC, and STATCOM) are compared for the voltage profile of each bus in this transmission system when only the reactive power load is increased to 50% of the base case. This plot only displays the method that was effective to enhance the deviation which was FPA in all devices when analyzing the base case. FPA, flower pollination algorithm.

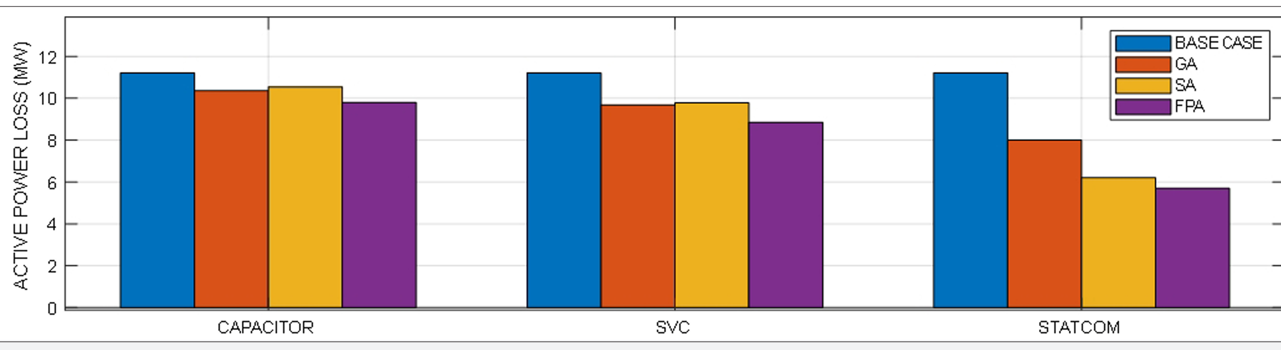

Fig. 12. Active power loss of base case. All three devices (capacitor, SVC, and STATCOM) are compared for the real power minimization in this transmission system of the base case. This plot only displays the method that was effective to minimize the power loss which was FPA in all devices when analyzing the base case.

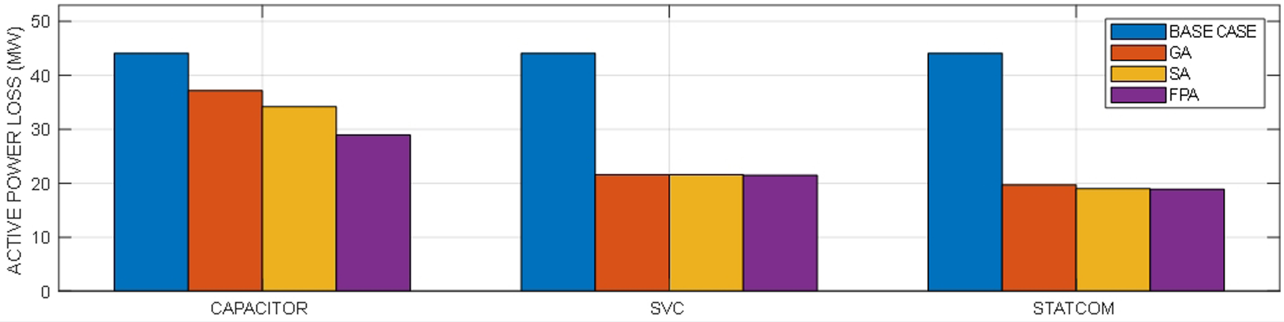

Fig. 13. Active power loss of 50% load increase. All three devices (capacitor, SVC, and STATCOM) are compared for the real power minimization in this transmission system when both real and reactive power load is increased to 50% of the base case. This plot only displays the method that was effective to enhance the deviation which was FPA in all devices when analyzing the base case. FPA, flower pollination algorithm.

As shown in Table IV, uniformly increasing both the real and reactive power of the load power to 50%, the loss was 44.1204 MW before the FACTS placement. After the placement of the capacitor at bus 8 using FPA, the loss was reduced to 28.9428 MW, but SVC placed at bus 24 further reduces it to 21.5091 MW with FPA. Comparing the work of STATCOM and SVC in Fig. 13, the reduction was not all that wide when 80 MVAr was injected to bus 29 with P_{loss} of 18.9033MW.

2) Case 2 (P_{load} Increase)

Only the load voltage's real power is increased to 50% of the base case, resulting in a total active power loss of 34.422 MW before the FACTS device is installed in Table V. After the placement of the device is shown in Fig. 14, there was a reduction of 8.4199 MW by placing the shunt capacitor at bus 24 and generating 113.713 MVAr at bus 24 with SVC reducing it from 34.4215 MW to 16.571 MW. With the characteristics of STATCOM used to increase the system capability, the losses were minimum at 13.7553 MW, and FPA ran all FACTS devices with the minimum losses.

3) Case 3 (Q_{load} Increase)

From Fig. 15, one could notice an increase in reactive power only on all load buses, which less influences the active power loss minimization. With a 50% increase in reactive power shown in Table VI, without

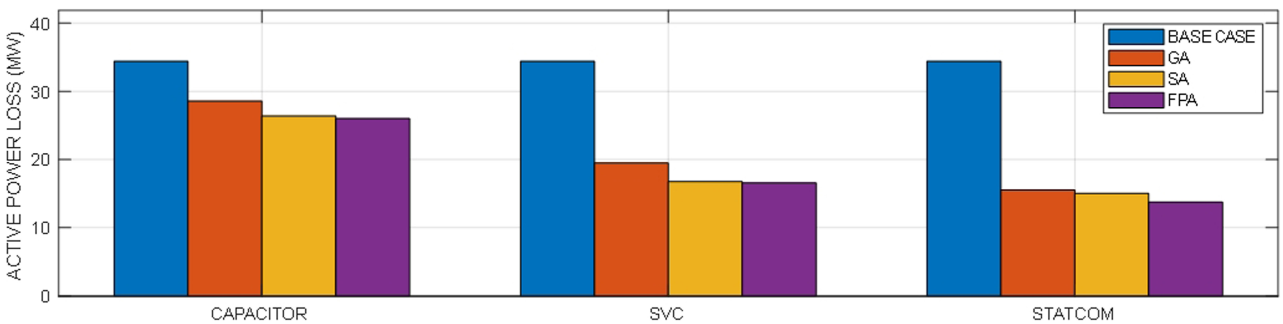

Fig 14. Active power loss of 50% P_{load} increase. All three devices (capacitor, SVC, and STATCOM) are compared for the real power minimization in this transmission system when only the real power load is increased to 50% of the base case. This plot only displays the method that was effective to enhance the deviation which was FPA in all devices when analyzing the base case.

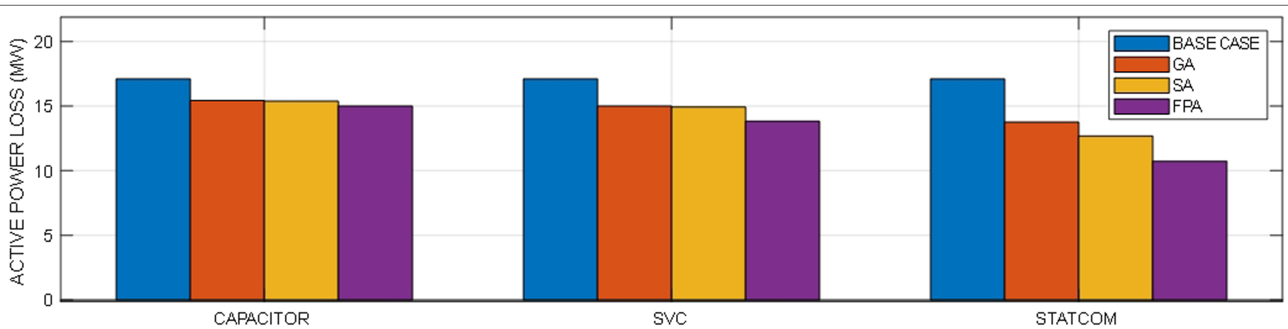

Fig. 15. Active power loss of 50% Q_{load} increase. All three devices (capacitor, SVC, and STATCOM) are compared for the real power minimization in this transmission system when only the reactive power load is increased to 50% of the base case. This plot only displays the method that was effective to enhance the deviation which was FPA in all devices when analyzing the base case. FPA, flower pollination algorithm.

the placement of the FACTS device, the active loss was 17.10405 MW. After installation, the capacitor's losses are reduced by 15.00 MW, the SVC's losses are reduced by 13.818 MW, and the STATCOM's losses are reduced by 10.731 MW.

VI. WILCOXON SIGNED-RANK TEST

This test compares two sets of data using a non-parametric statistical hypothesis test. The benefit of this test is that the information need not be usually distributed [28]. The tests efficiently compute the difference between paired data and look at this difference to see if it is statistically significant. It is used to contrast an alternative hypothesis with the null hypothesis, especially the assumption that one group often has higher values than the other, which is defined in (25) [29]:

$$H_0 : \mu = \mu_0$$
$$H_1 : \mu \neq \mu_0 \quad (25)$$

where μ is the base case bus voltages and μ_0 is the bus voltage after the placement of FACTS devices, with the level of significance (α) to be at 5% (0.05). The Wilcoxon signed-rank sum test probability is determined after placement of the FACTS devices with the use of the three-heuristic algorithm. Table VII TABLE VIII Table IX shows the probability (*P*) of the statistical Wilcoxon rank sum test for the PESCO bus system. From all the tables, the *P*-values of the FACTS devices are less than .05, so the null hypothesis is rejected. But STATCOM was having the smallest in each case, this is a strong evidence that by installing STATCOM, the voltages of the system are improved when compared to the original system. Therefore, it can be concluded that the results are statistically significant.

TABLE VII. WILCOXON TEST PROBABILITY FOR THE BASE CASE

	Case 1		
	Capacitor	SVC	STATCOM
P	3.2166e-07	2.7118e-07	2.4770e-07

TABLE VIII. WILCOXON TEST PROBABILITY FOR THE LOAD ACTIVE POWER INCREMENT

	Case 2		
	Capacitor	SVC	STATCOM
P	2.9491e-07	2.6092e-07	2.4770e-07

TABLE IX. WILCOXON TEST PROBABILITY FOR THE LOAD REACTIVE POWER INCREMENT

	Case 3		
	Capacitor	SVC	STATCOM
P	3.2566e-07	2.7527e-07	2.4770e-07

VII. CONCLUSION

In this paper, the shunt capacitor, SVC, and STATCOM devices were analyzed simultaneously to improve the voltage profile and minimize the total active power loss using the metaheuristic optimization (GA, SA, and FPA) approach for its placement and optimal sizing under various loading conditions. The proposed approach was tested on two test cases: PESCO 132 kV transmission system (Pakistan) with a consideration of load variation and IEEE 30 bus system where only the based case was considered to prove the effectiveness and validity of the proposed algorithm. The comparisons of the tabulated results obtained prove that in all cases, the proposed FPA algorithm performed better in both test system to enhance the voltage profile and minimizes the active power losses. However, SVC performed better than using a capacitor; but the use of STATCOM was more effective due to its better performance and faster response in maintaining the bus voltage magnitude and improving the system losses. The convergence curves of the IEEE system further support the superiority of the FPA algorithm over the other algorithms due to its faster convergence rate with fewer iterations.

Similarly, the total active power loss was minimal in all cases when the FPA was applied for optimization with the use of SVC and capacitor but STATCOM had the minimum real power losses. In conclusion, the results show that STATCOM has more control to enhance the voltage profile and minimization of the total active power loss using the FPA algorithm. The efficiency of the STATCOM device over the SVC and capacitor is proved through the statistical Wilcoxon test, even for various load variations.

Applications of the proposed approach on large-scale transmission power systems and series FACTS controllers are the future scope of this work.

Peer-review: Externally peer-reviewed.

Author Contributions: Concept – D.O.A.; Design – A.A.M.; Supervision – G.I.R.; Data Collection and/or Processing – H.H.; Analysis and/or Interpretation – D.O.A., A.A.M.; Literature Review – D.O.A., H.H.; Writing – D.O.A., A.A.M.; Critical Review – G.I.R.

Declaration of Interests: The author has no conflicts of interest to declare.

Funding: The author declared that this study has received no financial support.

REFERENCES

1. T. V. Cutsem and C. Vournas, *Voltage Stability of Electric Power Systems*. New York: Springer, 2008.
2. M. Gitizadeh and M. Kalantar, "A novel approach for optimum allocation of facts devices using multi-objective function," *Energy Convers. Manag.*, vol. 50, no. 3, pp. 682–690, 2009. [CrossRef]
3. B. Bhattacharyya, V. K. Gupta, and S. Kumar, "UPFC with series and shunt facts controllers for the economic operation of a power system," *Ain Shams Eng. J.*, vol. 5, no. 3, pp. 775–787, 2014. [CrossRef]
4. D. Divan *et al.*, "A distributed static series compensator system for realizing active power flow control on existing power lines," IEEE PES Power Systems Conference and Exposition, 2004., New York, NY, USA, vol. 2 pp. 654–661, 2004. [CrossRef]
5. A. A. Shehata, M. A. Tolba, A. M. El-Rifaie, and N. V. Korovkin, "Power System Operation Enhancement using a new hybrid methodology for optimal allocation of facts devices," *Energy Rep.*, vol. 8, pp. 217–238, 2022. [CrossRef]

6. D. Radu and Y. Besanger, “Blackout prevention by optimal insertion of facts devices in power systems,” 2005 International Conference on Future Power Systems, 2005. [CrossRef]
7. K. Kavitha and R. Neela, “Comparison of BBO, WIPSO & PSO techniques for the optimal placement of facts devices to enhance system security,” *Procedia Technol.*, vol. 25, pp. 824–837, 2016. [CrossRef]
8. M. Nadeem, M. Z. Zeb, K. Imran, and A. K. Janjua, “Optimal Sizing and Allocation of SVC and TCSC in Transmission Network by combined Sensitivity index and PSO,” 2019 International Conference on Applied and Engineering Mathematics (ICAEM), Taxila, Pakistan, 2019, pp. 111–116. [CrossRef]
9. N. R. Bujal, M. Sulaiman, A. F. Abd Kadir, T. Khatib, and N. Eltawil, “A comparison between GSA and IGSA for optimal allocation and sizing of DG and impact to voltage stability margin in electrical distribution system,” *J. Electr. Eng. Technol.*, vol. 16, no. 6, pp. 2949–2966, 2021. [CrossRef]
10. M. Ettappan, V. Vimala, S. Ramesh, and V. T. Kesavan, “Optimal reactive power dispatch for real power loss minimization and voltage stability enhancement using artificial bee colony algorithm,” *Microprocess. Microsyst.*, vol. 76, p. 103085, 2020. [CrossRef]
11. E. A. Belati, C. F. Nascimento, H. de Faria, E. H. Watanabe, and A. Padilha-Feltrin, “Allocation of static VAR compensator in electric power systems considering different load levels,” *J. Control Autom. Electr. Syst.*, vol. 30, no. 1, pp. 1–8, 2019. [CrossRef]
12. W. M. Villa-Acevedo, J. M. López-Lezama, D. G. Colomé, and J. Cepeda, “Long-term voltage stability monitoring of power system areas using a kernel extreme learning machine approach,” *Alex. Eng. J.*, vol. 61, no. 2, pp. 1353–1367, 2022. [CrossRef]
13. R.-A. Moradi, and R. Zeinali Davarani, “Introducing a new index to investigate voltage stability of power systems under actual operating conditions,” *Int. J. Electr. Power Energy Syst.*, vol. 136, p. 107637, 2022. [CrossRef]
14. A. A. Mohamed, S. Kamel, M. H. Hassan, M. I. Mosaad, and M. Aljohani, “Optimal Power Flow Analysis based on hybrid gradient-based optimizer with moth–flame optimization algorithm considering optimal placement and sizing of facts/wind power,” *Mathematics*, vol. 10, no. 3, p. 361, 2022. [CrossRef]
15. S. P. Dash, K. R. Subhashini, and J. K. Satapathy, “Optimal location and parametric settings of facts devices based on Jaya blended moth flame optimization for transmission loss minimization in power systems,” *Microsyst. Technol.*, vol. 26, no. 5, pp. 1543–1552, 2020. [CrossRef]
16. I. Kheirizad, A. Mohammadi, and M. H. Varahram, “A novel algorithm for optimal location of facts devices in power system planning,” *J. Electr. Eng. Technol.*, vol. 3, no. 2, pp. 177–183, 2008. [CrossRef]
17. R. M. Mathur and R. K. Varma, *Thyristor-Based Facts Controllers for Electrical Transmission Systems*. Chichester: Wiley, 2002.
18. X.-P. Zhang, E. Handschin, and M. Yao, “Multi-control functional static synchronous compensator (STATCOM) in power system steady-state operations,” *Electr. Power Syst. Res.*, vol. 72, no. 3, pp. 269–278, 2004. [CrossRef]
19. L. R. de Araujo, D. R. R. Penido, S. Carneiro, and J. L. R. Pereira, “Optimal unbalanced capacitor placement in distribution systems for voltage control and energy losses minimization,” *Electr. Power Syst. Res.*, vol. 154, pp. 110–121, 2018. [CrossRef]
20. J. H. Holland, *Adaptation in Natural and Artificial Systems: An Introductory Analysis with Applications to Biology, Control, and Artificial Intelligence*. Cambridge: The MIT Press, 1992.
21. X.-S. Yang, "Flower pollination algorithm for global optimization." International conference on unconventional computing and natural computation. Berlin, Heidelberg: Springer, 2012.
22. X.-S. Yang, and X. He, “Nature-inspired optimization algorithms in engineering: Overview and applications,”*Nature-Inspired Computation in Engineering*, 2016, pp. 1–20. [CrossRef]
23. X.-S. Yang, M. Karamanoglu, and X. He, “Multi-objective flower algorithm for optimization,” *Procedia Comput. Sci.*, vol. 18, pp. 861–868, 2013. [CrossRef]
24. M. -u. -N. Khursheed *et al.*, “Review of Flower Pollination Algorithm: Applications and Variants,” 2020 International Conference on Engineering and Emerging Technologies (ICEET), Lahore, Pakistan, 2020. pp. 1–6. [CrossRef]
25. M. N. Rosenbluth, A. H. Teller, and E. Teller, *Equation of State Calculations by Fast Computing Machines*. Metropolis: A. W. Rosenbluth, 1953.
26. S. Kirkpatrick, C. D. Gelatt, and M. P. Vecchi, “Optimization by simulated annealing,” *Science*, vol. 220, no. 4598, pp. 671–680, 1983. [CrossRef]
27. R. D. Zimmerman, and C. E. Murillo-Sanchez, *MATPOWER*, version 7.1 [Software], 2020. Available: https://matpower.org
28. H. Hizarci, O. Demirel, and B. E. Turkay, "Distribution network reconfiguration using time-varying acceleration coefficient assisted binary particle swarm optimization," *Eng. Sci. Technol. An Int. J.*, vol. 35, p. 101230, 2022. [CrossRef]
29. X. Zhang, and Shaochen Wen, "Heap-based optimizer based on three new updating strategies," *Expert Syst. Appl.*, vol. 209, p. 118222, 2022. [CrossRef]

Ghamgeen I. Rashed was born in Sulaimani, Iraq. He received the B.Sc. degree in electrical engineering from Salahaadin University, Iraq, in 1995, the M.Sc. degree from Sulaimani University, Iraq, in 2003, and the Ph.D. degree in power system and its automation from the Huazhong University of Science and Technology (HUST), China, in 2008. He is currently an Assistant Professor at the School of Electrical Engineering, Wuhan University, China. His special research interests include AI and its application to power systems, FACTS devices, especially TCSC and its control.

Otuo-Acheampong Duku was born in Kumasi City, Ashanti Region, Ghana. He received the higher National Diploma in Electrical and Electronic Engineering from Kumasi Technical University, in 2013, the B.Sc. degree in Electrical Engineering and Automation from China Three Gorges University, Yichang, China, in 2020. He is currently working toward the master's degree in Power System and Automation with the School of Electrical and Automation, Wuhan University, Wuhan, China. His current research interest is power system stability.

Amoh Mensah Akwasi received his bachelor's degree in Electrical Engineering and Automation from China Three Gorges University, China, in 2021. He is currently pursuing his master's degree in Electrical and Computer Engineering at the South China University of Technology, China. He worked as an Assistant Electrical Engineer at Guangdong Jinlong Company Limited in Dongguan, China. His research interest includes power system and its automation.

Hussain Haider was born in Vehari, Pakistan. He received his B.Sc. in Electrical Engineering and Technology from the Institute of Southern Punjab, Multan, Pakistan, in 2015, and his M.Sc. degree in Electrical Engineering from Wuhan University, China, in 2020 and now he is a Ph.D. scholar at the Smart Grid Research Institute at School of Electrical Engineering and Automation, Wuhan University, Hubei, China. His special research interest includes FACTS devices, in particular, TCSC, UPFC, and its control; power transmission networks; smart grids; demand side management; and Internet of things.